



# The University of Bradford Institutional Repository

<http://bradscholars.brad.ac.uk>

This work is made available online in accordance with publisher policies. Please refer to the repository record for this item and our Policy Document available from the repository home page for further information.

To see the final version of this work please visit the publisher's website. Access to the published online version may require a subscription.

**Link to publisher's version:** <http://dx.doi.org/10.1016/j.carbpol.2015.01.066>

**Citation:** Dul M, Paluch KJ, Kelly H, Healy AM, Sasse A and Tajber L (2015) Self-assembled carrageenan/protamine polyelectrolyte nanoplexes-Investigation of critical parameters governing their formation and characteristics. *Carbohydrate Polymers*. 123: 339-349.

**Copyright statement:** © 2015 Elsevier. Reproduced in accordance with the publisher's self-archiving policy. This manuscript version is made available under the [CC-BY-NC-ND 4.0 license](http://creativecommons.org/licenses/by-nc-nd/4.0/).



**Self-assembled carrageenan/protamine polyelectrolyte nanoplexes – investigation of critical parameters governing their formation and characteristics**

Maria Dul<sup>1</sup>, Krzysztof J. Paluch<sup>1,2</sup>, Hazel Kelly<sup>1</sup>, Anne Marie Healy<sup>1</sup>, Astrid Sasse<sup>1</sup>, Lidia Tajber<sup>1\*</sup>

\*To whom correspondence should be addressed: [lidia.tajber@tcd.ie](mailto:lidia.tajber@tcd.ie)

Phone: 00353 1 896 2787 Fax: 00353 1 896 2810

Affiliation:

1. School of Pharmacy and Pharmaceutical Sciences, Trinity College Dublin, Dublin 2, Ireland.

2. Bradford School of Pharmacy, School of Life Sciences, Centre for Pharmaceutical Engineering Science, University of Bradford, Norcroft Building, Richmond Road, Bradford W. Yorks, BD7 1DP, UK.

Email addresses of authors:

Maria Dul – [mdul@tcd.ie](mailto:mdul@tcd.ie)

Krzysztof J. Paluch - [K.J.Paluch@bradford.ac.uk](mailto:K.J.Paluch@bradford.ac.uk)

Hazel Kelly – [hakelly@tcd.ie](mailto:hakelly@tcd.ie)

Anne Marie Healy – [healyam@tcd.ie](mailto:healyam@tcd.ie)

Astrid Sasse - [sassea@tcd.ie](mailto:sassea@tcd.ie)

Lidia Tajber – [lidia.tajber@tcd.ie](mailto:lidia.tajber@tcd.ie)

## Abstract

1 The aim of this work was to investigate the feasibility of cross-linker free polyelectrolyte  
2 complex formation at the nanoscale between carrageenan (CAR) and protamine (PROT).  
3 The properties of CAR/PROT nanoparticles (NPs) were dependent on the carrageenan type:  
4 kappa (KC), iota (IC) and lambda (LC), concentration of components, addition of divalent  
5 cations, weight mixing ratio (WMR) of constituents and mode of component addition. In the  
6 case of 0.1% w/v solutions, IC-based NPs had the smallest particle sizes (100-150 nm) and  
7 low polydispersity indices (0.1-0.4). A decrease in the solution concentration from 0.1% to  
8 0.05% w/v enabled the formation of KC/PROT NPs. All carrageenans exhibited the ability to  
9 form NPs with surface charge ranging from -190 to 40 mV. The inclusion of divalent cations  
10 caused an increase in the particle size and zeta potential. Infrared analysis confirmed the  
11 presence of a complex between CAR and PROT and showed that IC chains undergo  
12 structural changes when forming NPs. Colloidal stability of NPs was related to the initial  
13 surface charge of particles and was time- and pH-dependent. IC was found to be the most  
14 suitable type of CAR when forming nanoplexes with PROT.

15

16 **Keywords:** Carrageenan; Protamine; Nanoparticles; Polyelectrolyte Complexes; Dynamic  
17 Light Scattering; Infrared spectroscopy

## 18 **1. Introduction**

19 Recent advances in pharmaceutical nanotechnology are focused on using polymeric  
20 nanoparticulate systems as carriers for drugs (Delie & Blanco-Prieto, 2005). Nanoparticles  
21 (NPs) formulated from natural polymers have attracted considerable interest (Hans &  
22 Lowman, 2002). NPs have many advantages, such as the potential to retain protein stability,  
23 increase duration of therapeutic effects of proteins and they can be administered by  
24 nonparenteral routes (Sarmiento, Bibeiro, Veiga, Ferreira and Neufeld, 2007). Natural  
25 polymers extensively studied for drug delivery purposes include polysaccharides such as  
26 alginate, chitosan, carrageenan (CAR) and proteins, for example casein and gelatin (Sonia &  
27 Sharma, 2012).

28 Polymers, especially those of natural origin, are often composed of subunits capable of  
29 bearing charge, thus the polyelectrolyte complexation method of NP preparation has  
30 received increasing attention in recent years. NPs formed by this method have several  
31 characteristic advantages for cellular uptake and colloidal stability, including suitable  
32 diameter, surface charge, spherical morphologies and low polydispersity indices (Bayat et  
33 al., 2008). Furthermore, the preparation of NPs by polyelectrolyte complexation methods can  
34 be carried out in completely aqueous conditions and at ambient temperature; therefore the  
35 stability and biological activity of loaded peptides would not be affected (Hu, Yang and Hu,  
36 2012; Ryan et al., 2013; Umerska et al., 2012, 2014).

37 Carrageenans (CARs) are an example of such polymers and are capable of forming  
38 polyanions. They are a family of hydrophilic sulphated biopolysaccharides extracted from  
39 various species of the *Rhodophyta* class of red seaweeds (Campo, Kawano, Braz da Silva  
40 and Carvalho, 2009). CARs are composed of a hydrophilic linear sulphated backbone of  
41 alternating 1→3 glycosidic-linked β-D-galactopyranose units and 1→4 glycosidic-linked α-D-  
42 galactopyranose units or 1→4 glycosidic-linked 3, 6-anhydro-α-D-galactopyranose units  
43 (Figure 1) (Berth, Vukovic and Lechner, 2008) and principally differ in the number and  
44 position of the sulphate groups, however these reflect only general differences in the  
45 composition and degree of sulphation (Necas & Bartosikova, 2013). The actual content of the

46 sulphate residue (by weight) may vary between 15 and 40% for the various carrageenan types  
47 (Nanaki, Karavas, Kalantzi and Bikiaris, 2010). Their applications include experimental  
48 medicine, pharmaceutical formulations and are well established as gelling, stabilising and  
49 thickening agents for food, cosmetics and industrial uses (Necas & Bartosikova, 2013).  
50 CARs are biocompatible and biodegradable polysaccharides with low toxicity and well  
51 documented properties of controlling and extending release of various drug substances  
52 (Nanaki et al., 2010) as well as improving apparent solubility and dissolution rates of poorly  
53 soluble actives (Dai, Dong and Song, 2007). In addition, studies have shown that CARs  
54 have a high capacity to interact with proteins due to their strong ionic nature (Malafaya, Silva  
55 and Reis, 2007) and form excellent matrices for predictable synthesis of magnetite  
56 nanoparticles (Daniel-da-Silva et al., 2007).

57 To form polyelectrolyte complexes (PECs) with CAR, protamine (PROT) was selected due to  
58 its reported *in vitro* membrane-translocating ability, believed to be associated with its positively  
59 charged polyarginine chains (Reynolds, Weissleder and Josephson, 2005). The use of cell-  
60 penetrating peptides for drug delivery has been extensively studied over the past two  
61 decades (Temsamani & Vidal, 2004).

62 Shumilina and Shchipunov (2002) investigated interactions between CAR and chitosan (CS).  
63 They showed that the nature or type of CAR considerably influenced the characteristics of  
64 the PECs. The mechanical strength of PEC gels were ranked as follows: lambda  
65 carrageenan (LC)/CS > iota carrageenan (IC)/CS > kappa carrageenan (KC)/CS. Moreover,  
66 the gels obtained with IC and KC were temperature sensitive due to the helix-coil  
67 conformational transitions in their molecules (Shumilina & Shchipunov, 2002). An  
68 investigation was performed on the potential of PECs formed between KC, IC or LC and CS  
69 to form controlled release systems for glucose oxidase (Briones & Sato, 2010). The complex  
70 between CS and KC showed high encapsulation efficiencies for glucose oxidase while  
71 having the lowest release rate for this compound. Furthermore, this complex was able to  
72 protect the encapsulated glucose oxidase against degradation in pH 1.2 solution, in a  
73 chitosanase solution and in a pepsin solution (Briones & Sato, 2010). Another example of

74 CS/CAR PECs used for delivery of proteins has been reported (Li, Hein and Wang, 2013).  
75 As characterised by Li et al. (2013), in acidic solution the negatively charged sulphate  
76 groups of KC bound to positively charged amino groups of CS and formed acid-base PECs.  
77 When the pH was increased, amino groups protonated and the binding activity between both  
78 components became weaker, which resulted in swelling and disintegration of PEC and finally  
79 release of the protein. Modulation of drug release to the target site was possible by adjusting  
80 the factors that cause swelling properties of PEC (Li et al., 2013).

81 A number of publications show that carrageenans complex to CS (Briones & Sato, 2010; Li  
82 et al. 2013; Shumilina & Shchipunov, 2002), however no work has been published to date  
83 which indicates whether complexation between CAR and PROT is possible. Previous work  
84 by Umerska et al. (2014) showed that PROT/hyaluronate PECs can form, at the nanoscale,  
85 but depending on the ratio of constituents in such PECs their colloidal stability varies  
86 considerably. Therefore in this study we have focused on CAR/PROT systems with the aim  
87 of undertaking a methodical assessment of the various types of CAR, their concentration,  
88 weight mixing ratios, mode of preparation and the additional small cation addition during  
89 PECs formation to investigate if CAR/PROT nanoplexes can be obtained and to determine  
90 the characteristics of any such nanoplexes formed. CAR/PROT nanoplexes have the  
91 potential of being biocompatible, safe as well as capable of peptide binding and protection,  
92 as demonstrated for hyaluronate/PROT systems (Umerska et al., 2014), however key  
93 parameters determining their pharmaceutical suitability (such as optimum conditions of  
94 formation and stability) first need to be assessed.

95

## 96 **2. Materials and methods**

### 97 **2.1 Materials**

98 Iota carrageenan (IC, cat. no. C4014), kappa carrageenan (KC, cat. no. 22048), lambda  
99 carrageenan (LC, cat. no. 22049) and protamine (PROT) (as a sulphate salt, from salmon,  
100 cat. no. P4020) were obtained from Sigma-Aldrich. All other reagents and chemicals used  
101 were of analytical grade.

## 102 **2.2 Preparation and characterisation of polymer and PROT solutions**

103 Loss on drying for polymers was determined by thermogravimetry. A Mettler TG 50 module  
104 linked to a Mettler MT5 balance was employed (Paluch et al., 2010). Sample weights  
105 between 10–12 mg were used, placed into open aluminium pans and heated isothermally for  
106 3h at 105 °C under nitrogen purge.

107 Sulphate content was measured by turbidimetry on 20 mg polymer samples hydrolysed for  
108 5h in 15 ml HCl at 105 °C in sealed glass tubes, following the procedure of Dogson and  
109 Price (1962). Aliquots of 0.2 ml of the hydrolyses were transferred to glass tubes containing  
110 3.8 ml 3% w/v trichloroacetic acid and 1 ml of the barium chloride reagent (0.5 g barium  
111 chloride dissolved in 100 ml of 0.5% w/v gelatin solution) was added to each of the tubes.  
112 The contents were thoroughly mixed, kept at room temperature for 15-20 minutes and  
113 absorbance was measured at 360 nm against the blank. The blank consisted of 0.2 ml 1M  
114 HCl mixed with 3.8 ml 3% w/v trichloroacetic acid and 1 ml of gelatin solution. The calibration  
115 curve was made using anhydrous potassium sulphate (20-200 µg/ml sulphates).

116 Aliquots of 100 ml of 0.1% w/v (1 mg/ml) and 0.05% w/v (0.5 mg/ml) solutions of IC, KC, LC  
117 and PROT were prepared in deionised water. LC and PROT were dispersed at 25 °C and  
118 stirred for 30 min on a magnetic stirrer at 500 rpm until a clear solution resulted. For KC and  
119 IC, the polymers were first dissolved with vigorous stirring in deionised water at 80 °C. When  
120 clear solutions were obtained, the polymer solutions were removed from the heat and stirred  
121 at 500 rpm for at least 30 min until the temperature reached 25 °C. The volume of KC and IC  
122 solutions was made up to 100 ml to account for any evaporation which occurred during the  
123 heating.

124 A low frequency vibration viscometer (SV-10 Vibro Viscometer, A&D Company Limited,  
125 Japan) was employed to measure the viscosity of polymer solutions and NP dispersions.  
126 The viscometer was calibrated with deionised water before use. Viscosity measurement of  
127 each sample was carried out in triplicate at 25±0.2 °C. A water bath (Reciprocal Shaking  
128 Bath Model 25, Precision Scientific, UK) was used to equilibrate the samples prior to the  
129 measurement. The results are given as an average ± standard deviation (SD).

130 A Thermo Electron Orion 420A<sup>+</sup> Basic pH/mV/ORP 25 °C, Thermo Electron Corporation pH  
131 meter equipped with an Orion Rose™ 8103SC glass body pH semi-micro electrode was  
132 used to perform pH analyses. pH measurement of each sample was conducted in triplicate  
133 at 25 °C. The pH meter was calibrated with standard buffer solutions at pH 4, 7 and 10  
134 before each batch of sample measurements. The results are given as an average value of  
135 three measurements ± SD.

136 Gel Permeation Chromatography (GPC) measurements of the molecular weight of  
137 carrageenans were performed using a system composed of an LC-10 AT VD liquid  
138 chromatograph pump system, a SIL-10 AD VP autoinjector, a FCV-10 AL VP low pressure  
139 gradient flow-control valve, a DGU-14A degasser, a Waters 410 refractive index detector  
140 and an SCL-10A VP system controller (Shimadzu, Japan). A Plaquagel–OH mixed 8 µm,  
141 300 × 7.5 mm column (Polymer Laboratories Ltd., UK) was used. The mobile phase was  
142 composed of 0.2M NaCl and 0.01M NaH<sub>2</sub>PO<sub>4</sub> adjusted to pH 7.4 with NaOH solution  
143 (Umerska et al., 2012). The mobile phase flow rate in each case was 1 ml/min. Pullulan  
144 standards (PL Polymer Laboratoires, Germany) were used to construct the calibration curve.  
145 Solutions of standards and samples (1 mg/ml) were prepared in the mobile phase and 100 µl  
146 of samples or standards were injected in triplicate. Shimadzu CLASS-VP software (version  
147 6.10) with GPC for Class VP (version 1.02) was used for data collection and peak  
148 integration.

149 Fourier transform infrared spectroscopy (FTIR) of various types of carrageenans and PROT  
150 was carried out as described previously (Umerska et al., 2012).

### 151 **2.3 Synthesis and characterisation of NPs composed of CAR and PROT**

152 Aliquots of 0.05% and 0.1% w/v solutions of IC, KC, LC and PROT were prepared according  
153 to the method described in Section 2.2. Polymer and PROT solutions were combined  
154 together in various v/v ratios at room temperature (RT) and mixed under magnetic stirring for  
155 around 10 min to allow stabilisation of the system. Since the concentration of both  
156 components was the same, either 0.05% or 0.1% w/v, those v/v ratios were equivalent to  
157 CAR/PROT weight mixing ratios (WMRs) and WMRs are used throughout this manuscript.



158 Two methods of NP preparation were considered:

159 Method\_A. An aliquot of PROT solution was added to an aliquot of polymer solution under  
160 magnetic stirring. Stirring was continued for 10 minutes.

161 Method\_B. An aliquot of polymer solution was introduced to an aliquot of PROT solution  
162 under magnetic stirring. Stirring was continued for 10 minutes.

163 To examine the impact of divalent cations on IC/PROT NPs formation, CaCl<sub>2</sub> (final  
164 concentration of 0.05 M and 0.01 M) and ZnCl<sub>2</sub> (final concentration of 0.01 M) were  
165 dissolved in 0.1% w/v solution of PROT. The polymer and PROT/cation solutions were  
166 combined together in various v/v ratios at room temperature and mixed under magnetic  
167 stirring for 10 minutes to allow stabilisation of the system.

#### 168 **2.4 Physicochemical characterisation of NPs**

169 The mean particle size (hydrodynamic particle diameter) and polydispersity index (PDI) of  
170 prepared polyelectrolyte complexes were determined by dynamic light scattering (DLS) with  
171 the use of 173 degrees backscatter detection. The value of material refractive index used  
172 was 1.59, while that of absorption 0.01. Actual values of medium viscosity were input and  
173 the refractive index of dispersant was kept 1.33, the same as water. The electrophoretic  
174 mobility values measured by Laser Doppler Velocimetry (LDV) were converted to zeta  
175 potential (ZP) values using the Smoluchowski equation. Both measurements (DLS and LDV)  
176 were performed on a Zetasizer Nano ZS series Nano-ZS ZEN3600 fitted with a 633 nm laser  
177 (Malvern Instruments Ltd., UK). Samples without dilutions were placed directly into a clear  
178 plastic zeta cell (DTS 1061, Malvern, UK) and equilibrated for 2 min at 25 °C prior to the  
179 measurement. The readings for each sample were performed at least three times and at  
180 least three batches of each sample were prepared and analysed. The results are presented  
181 as an average of size  $\pm$  SD, polydispersity index (PDI)  $\pm$  SD and ZP  $\pm$  SD.

182 Viscosity and pH measurements were performed in the same way as described above in  
183 Section 2.2.

184 FTIR analysis was performed on CAR/PROT systems produced by combining 0.1% w/v  
185 solutions at a weight mixing ratio of 1 as described previously (Umerska et al., 2012).

186 The structural and morphological analysis of NPs was performed by transmission electron  
187 microscopy (TEM) and scanning electron microscopy (SEM). TEM was carried out with a  
188 Tecnai G<sup>2</sup> 20 TWIN microscope (FEI, USA). Samples were applied to the shiny side of the  
189 grid for 30 s and the excess of sample was removed by blotting the grid with a filter paper.  
190 Prepared samples were dried for 24h under ambient conditions. SEM was carried out with a  
191 Zeiss Supra Variable Pressure Field Emission Scanning Electron Microscope (Germany)  
192 equipped with a secondary electron detector. Liquid dispersions of NPs were directly placed  
193 onto aluminium stubs and dried for 24h in a desiccator over silica gel. Dried NPs were  
194 sputter-coated with gold under vacuum prior to the analysis.

195 Physical (colloidal) stability of NP formulations was visually inspected immediately after  
196 preparation, prior to carrying out any measurements. The presence/absence of aggregation  
197 was recorded. The colloidal stability of NPs (in native dispersions) upon storage was  
198 determined by measuring changes in the hydrodynamic particle size, Pdl and ZP over time.  
199 Measurements and visual observations were performed directly after sample preparation  
200 (day 0) and were continued every 24h for a further 3 days.

201 The colloidal, physical stability of NPs in the following liquid media: 0.01M HCl, 0.1M acetate  
202 buffer pH 4.5, 0.1M 4-(2-hydroxyethyl)-1-piperazineethanesulfonic acid (HEPES) buffer pH  
203 6.5 and 0.01M phosphate buffered saline (PBS) pH 7.4 was also determined. The aqueous  
204 dispersions of NPs were diluted with a suitable medium in the 1:1 v/v ratio. The colloidal  
205 stability of the prepared NPs was determined by measuring changes in the mean  
206 hydrodynamic particle size over time. Measurements and visual observations were  
207 performed directly after sample preparation (day 0) and were continued every 24h for  
208 another 3 days.

## 209 **2.5 Statistical analysis**

210 The statistical significance of the differences between samples was determined by one-way  
211 analysis of variance (ANOVA) using Origin software version 7.5.

212

## 213 **3 Results and discussion**

## 214 **3.1 Formulation of NPs composed of various types of carrageenan and PROT**

### 215 **3.1.1 Impact of carrageenan type and solution concentration on NP formation**

216 The molecular weight of the polymers was determined by GPC and it ranged from ~600 to  
217 ~700 kDa (Table 1). It was therefore assumed that only differences in the polymer chemical  
218 composition and/or structural differences (Figure 1), but not molecular weight, may affect the  
219 NP formation. The molecular weight of the polymer is reported as a crucial parameter that  
220 determines the success of the polymeric NP formation process, as established by Boddohi,  
221 Killingsworth and Kipper (2008) and Umerska et al. (2012).

222 Preliminary studies were first executed to examine each type of CAR for its ability to form  
223 PECs with PROT. CAR and PROT solutions (each at 1 mg/ml) were combined at various  
224 CAR/PROT WMRs using manufacturing Method\_A, as previously employed by Umerska et  
225 al. (2012). The combination of IC and PROT gave the smallest particles with the lowest Pdl  
226 when compared with the KC/PROT and LC/PROT systems (Figure 2A and 2B). The particle  
227 size and Pdl were seen to increase with increasing CAR/PROT WMR. Formation of large  
228 particulates, an indication of coagulation or aggregation, was observed for most of the  
229 KC/PROT WMRs tested (Figure 2A). High Pdl values were measured for the KC/PROT  
230 samples with particles in the nano size range (Figure 2B). SEM analysis (Figure 3) showed  
231 the presence of NPs and not microparticles, thus it may be concluded that the appearance of  
232 large particles for some of the KC/PROT systems was symptomatic of an aggregation  
233 process rather than coagulation. NPs with particle sizes of ~100-350 nm were formed when  
234 combining LC and PROT solutions (Figure 2A). Generally, LC/PROT NPs were larger in size  
235 when the LC/PROT WMRs was lower than 1.

236 All combinations tested: KC/PROT, IC/PROT and LC/PROT showed the formation of large  
237 entities at a WMR of 1, consistent with charge neutralisation occurring at this CAR/PROT  
238 WMR (Boddohi et al., 2008; Umerska et al., 2012). This was an interesting finding, as the  
239 different types of CAR vary in the number of sulphate residues in their structures (Figure 1)  
240 and in theory each of them should have a different, characteristic charge neutralisation point.  
241 Nevertheless, the actual sulphate content in the various CAR types varied between 20 and

242 27% (Table 1), which can be considered similar. Since the pKa value of the anionic sulphate  
243 group in CAR is around 2 (Gu, Decker and McClements, 2004), at pH of the CAR solution  
244 (Table 1) ionisation of the sulphate groups should be complete and all the groups will be  
245 available for potential binding with PROT.

246 Zeta potential (ZP) values showed that the NPs can bear either negative or positive surface  
247 charge (Figure 2C). ZP of positively charged NPs had similar values for each type of NP,  
248 possibly due to the PROT presence on the surface. Negatively charged NPs composed of  
249 KC/PROT and LC/PROT had similar ZP values (around -100 mV at a CAR/PROT WMR of 3  
250 and approximately -200 mV at a CAR/PROT WMR of 5). A higher charge, around -80 - -100  
251 mV, in comparison to KC/PROT and LC/PROT, was measured for negatively charged  
252 IC/PROT NPs. NPs based on IC displayed the most promising results in terms of obtaining  
253 NPs with the smallest particle sizes and lowest Pdl values (Figure 2).

254 Thrimawithana, Young, Dunstan and Alany (2010) have characterised properties of  
255 carrageenan gels and reported the existence of both KC and IC as random coils in solution  
256 and at high temperatures. On reduction of this temperature a double-helix structure is  
257 induced to form small independent domains via intermolecular interactions between a limited  
258 number of polysaccharide chains. KC forms honeycomb-like, hard gel structures while IC  
259 forms soft, elastic gel structures (Thrimawithana et al., 2010). LC does not form gels and it is  
260 characterised by a random distribution of polymer chains in solution (Berth et al., 2008).  
261 Conformation dependent interactions of carrageenans with other polymers and drugs have  
262 been reported in the literature. Thrimawithana, Young, Bunt, Geen, and Alany (2011)  
263 highlighted that, in the coiled conformation, the sulphate groups of carrageenans are further  
264 apart (at a distance of about 1 nm) than in the helix conformation (about 0.66 nm). As such,  
265 long range intermolecular forces between the sulphate groups are weaker in the coiled  
266 formation. Therefore, the polyanionic character of carrageenans would appear more  
267 important for polyelectrolyte complexation when present in the helix form and inducing this  
268 helix conformation of CAR polymers when interacting with the polycation PROT would  
269 appear to be most desirable for NP formulation via polyelectrolyte complexation.

270 KC was seen as the most problematic of the polymers used in initial formulation studies  
271 using 1 mg/ml CAR solutions, with large, aggregated particles being produced at almost all  
272 KC/PROT weight ratios studied (Figure 2). A lower concentration, 0.5 mg/ml, of KC and  
273 PROT solutions was investigated and allowed the formation of particulates in the nano size  
274 range for all weight mixing ratios tested (Figure 2A). The NPs had lower Pdl values ranging  
275 from 0.21 to 0.46 and greater ZP values in comparison to the NP counterparts, if formed,  
276 made of 1 mg/ml solutions. While it was possible to obtain NPs based on KC when lowering  
277 its concentration, it is important to note that previous reports in the literature have indicated  
278 that typically a greater association efficiency of the drug can be achieved when greater  
279 concentration of polymers is used in their formulation (Sarmiento, Ribeiro, Veiga and  
280 Ferreira, 2006; Gupta and Karar, 2011). Thus NPs with a total polymer content of 1 mg/ml  
281 would be most desirable in terms of future studies on drug loading.

282 Overall, the CAR conformation in solution and its solution concentration appear to be the key  
283 determinants of success when forming polyelectrolyte nanoplexes with PROT. IC showed  
284 the most promising characteristics and small, homogenous and bearing either negative or  
285 positive surface charge NPs were successfully formed at 1 mg/ml solution concentrations.  
286 Additionally, it should be noted that amines (PROT is rich in arginine moieties) can induce  
287 ionic gelation of IC (Yeo, Baek and Park, 2001).

### 288 **3.1.2 Impact of the preparation method on properties of NPs**

289 Polyion addition mode is known to govern properties of polyelectrolyte nanoplexes (Chen,  
290 Heitmann and Hubbe, 2003; Dragan, Mihai and Schwarz, 2006; Birch & Schiffman, 2014). In  
291 experiments described in the previous section Method\_A (an aliquot of PROT solution was  
292 added to a volume of HA solution) was used. A method involving the reverse addition of  
293 components (a volume of PROT solution introduced to a volume of PROT solution), i.e.  
294 Method\_B, was also tested on KC/PROT (with a total polymer content of 0.5 mg/ml) and  
295 IC/PROT (with a total polymer content of 1 mg/ml) systems.

296 Preparation Method\_A yielded NPs that were generally smaller in size and with lower Pdl  
297 values in case of negatively charged NPs (a CAR/PROT WMR of 5, Figure 4A and B) than

298 those generated using Method\_B. Also, Method\_A allowed the formation of NPs at a  
299 CAR/PROT WMR of 2, while Method\_B resulted in samples containing large particles at this  
300 WMR. Statistically significant differences between the size of NPs were also observed for  
301 KC/PROT and IC/PROT at CAR/PROT WMRs of 0.2 and 0.5, but it was Method\_B that gave  
302 smaller NPs for IC/PROT while Method\_A resulted in smaller NPs for KC/PROT (Figure 4A).  
303 The variation in the particle size and Pdl was not reflected in similar changes in dynamic  
304 viscosity and ZP values (Figure 4C and D), and no general trends were discerned.

305 Birch and Schiffman (2014) investigated the order of solution addition, when making  
306 chitosan and pectin polyelectrolyte nanoplexes. Substantial differences in particle sizes and  
307 ZP values were seen, but the mechanism rationalising the variation was not provided.

308 Dragan et al. found that the charge neutralisation point of the complexes formed between  
309 acrylamide or methacrylate derivatives of poly(sulphonate)s and poly(quaternary amine)s  
310 was dependent on whether the titrant was the polyanion or polycation (Dragan et al., 2006).  
311 In all cases when the polycation was added to the polyanion, the molar charge ratio between  
312 the cationic and anionic species was shifted to higher values. This behaviour was explained  
313 by the charge localisation on the polycations, making them less efficient in the stabilisation of  
314 complex particles with the polyanion; thus larger in size aggregates were formed. The  
315 findings of Dragan et al. (2006) can be translated into the observed increase in the particle  
316 size of IC/PROT and KC/PROT NPs at a CAR/PROT WMP of 5 as well as KC/PROT at a  
317 CAR/PROT WMP of 0.2 and 0.5, when much larger particles, indicative of a looser structure  
318 and weaker species interactions, were formed using Method\_B (Figure 4A and D). Also,  
319 Method\_A permitted successful NP production at a CAR/PROT WMP of 2, while extensive  
320 aggregation was seen for Method\_B.

321 However, Method\_B yielded smaller particles, and with lower ZP values, for IC/PROT WMRs  
322 of 0.2 and 0.5, in comparison to Method\_A, so the supposition of lower polycation efficiency  
323 does not hold for these samples.

324 Umerska et al. highlighted the importance of the molecular weight ratio of the polyanionic  
325 and polycationic constituents and the difference in charge density (Umerska et al., 2014).

326 While it was possible to prepare NPs composed of hyaluronic acid (HA, molecular weight  
327 ~260 kDa) and PROT (molecular weight ~5 kDa), they were not physically stable and  
328 aggregated within hours due to the large difference in molecular weight of HA and PROT.  
329 Interestingly, the molecular weight ratio for KC/PROT is ~130 and that for IC/PROT ~140,  
330 yet physically stable NPs were formed (for stability data see Section 3.4). As IC is a much  
331 stronger polyanion than HA (Cundall, Lawton, Murray and Phillips, 1979) it is able to form  
332 stronger complexes with PROT, but strong, linear polyelectrolytes are also known to form  
333 stable, however non-stoichiometric complexes (Chen et al., 2003). The component in excess  
334 here, PROT, is expected to charge-stabilise the IC/PROT NPs.

335 The final conclusion is that PROT can either stabilise or destabilise NPs depending on the  
336 mode of mixing and the type of carrageenan. Practically, considering the rather small  
337 differences in NP properties depending on the use of Method\_A or Method\_B for the  
338 positively charge particles, Method\_A was selected for further experiments.

### 339 **3.1.3 Impact of Ca<sup>2+</sup> and Zn<sup>2+</sup> on NP formation**

340 Calcium ion has been widely used to crosslink negatively charged polysaccharides to aid NP  
341 formation and to promote better size distribution and polydispersity of formed (Liu, Jiao,  
342 Wang, Zhou and Zhang, 2008). As reported, Ca<sup>2+</sup> ions favour IC gel formation while K<sup>+</sup> ions  
343 favour KC gel formation (Thrimawithana et al., 2010). Thus the addition of divalent cations  
344 (Ca<sup>2+</sup> and Zn<sup>2+</sup>) was tested for possible alteration of IC/PROT NPs properties.

345 At first, Ca<sup>2+</sup> at a concentration of 0.05M was tested. However, only micron sized particles  
346 were formed after incorporation of Ca<sup>2+</sup> ions to the IC/PROT formulations. To further check  
347 the impact of Ca<sup>2+</sup> concentration, the concentration was decreased to 0.01M. This decrease  
348 in the ion concentration brought the particle size of PECs which were formed back into the  
349 nano-range (Figure 5A), however Pdl values were greater in comparison to those of  
350 formulations without Ca<sup>2+</sup> (Figure 5B). To further optimise the formulation another ion was  
351 sought. The presence of Zn<sup>2+</sup> ions at a concentration of 0.01M resulted in NPs with smaller  
352 particle sizes than those containing Ca<sup>2+</sup> ions (Figure 5A). However, the size of NPs formed  
353 with the divalent cation addition was still larger than formulations without ions (Figures 2A

354 and 5A). As expected, additional cations present in formulations resulted in lowering ZP for  
355 all weight ratios tested due to reaction with the anionic sulphate groups of the polymer  
356 (Figure 5C).

### 357 **3.2. Characterisation of interactions between CAR and PROT**

358 FTIR spectra of the different carrageenans, PROT and NPs, along with band assignments  
359 for the NP components, are presented in Figure 6. The identity of KC, IC and LC could be  
360 easily distinguished by the presence and location of bands of sulphate galactose and  
361 sulphate 3,6-anhydrogalactose (Figure 6). The FTIR spectra of NPs were dominated by  
362 vibrations characteristic of CAR in the 650-1400  $\text{cm}^{-1}$  region with prominent amide I and II  
363 peaks of PROT appearing between 1400 and 1700  $\text{cm}^{-1}$  confirming the presence of both  
364 components in the NP formulations.

365 No new covalent bonds were created in the process of combining CAR and PROT, but shifts  
366 of some absorption bands were evident (Table 2). Interestingly, the peaks associated with  
367 sulphate and amine groups of CAR and PROT moved substantially for KC/PROT and  
368 LC/PROT systems, while, for the IC/PROT sample, only the amide I band shifted  
369 considerably and not the sulphate bands. This implies that the various CAR types may  
370 interact with PROT via different mechanisms. Large shifts in the amide I band of chitosan  
371 were observed for chitosan/HA (Umerska et al., 2012) and chitosan/KC (Li et al., 2013)  
372 systems and attributed to the formation of a polyelectrolyte complex. Therefore it appears  
373 that all types of CAR are able to electrostatically complex with PROT, and this mechanism is  
374 dominant for KC/PROT and LC/PROT systems, but another process is also likely to occur in  
375 the case of IC/PROT. Thrimawithana et al. (2011) noticed that the region between 1000 and  
376 1200  $\text{cm}^{-1}$  is the most sensitive to structural changes of CAR as it shows stretching  
377 absorption bands of C-O-C and C-O bonds of the polysaccharides. There is a shift by 6  $\text{cm}^{-1}$   
378 of the absorption band located at 1155  $\text{cm}^{-1}$  towards higher wavenumbers for IC/PROT  
379 (shifts by 1-2  $\text{cm}^{-1}$  in the opposite direction are seen for KC- and LC-/PROT), consistent with  
380 deformation of IC polysaccharide chains. As the driving force for formation of PECs is  
381 attraction of oppositely charged moieties (already discussed above) and/or an increase in



382 entropy when the complexation is accompanied by release of counterions (Chen et al.,  
383 2003), the shift of the  $1155\text{ cm}^{-1}$  band may signify that the latter mechanism is also present  
384 and contributes to the formation of small and homogenous NPs.

### 385 **3.3. Structure and morphology of NPs**

386 Figure 3 shows SEM images of a range of CAR/PROT NPs. It can be observed that NPs  
387 with positive surface charge (a CAR/PROT WMR of 0.33) were generally spherical in shape  
388 and well defined (KC/PROT and IC/PROT), with the exception of LC/PROT for which a  
389 rather fused mass of very small nanoparticulates with sizes of approximately 10-50 nm was  
390 observed. It is therefore likely that data presented in Figure 2A pertains to aggregated  
391 LC/PROT NPs rather than individual particles. At a CAR/PROT WMR of 3 the particles were  
392 still approximately spherical, but a greater degree of fusion was apparent.

393 TE micrographs (Figure 3G and 3H) show spherical and well-defined structures. There is  
394 some of the polymeric corona effect (Umerska et al., 2012) visible for the NPs.

### 395 **3.4 Colloidal stability of IC/PROT NPs**

396 A range of formulations with different IC/PROT WMRs and properties were chosen for  
397 colloidal stability testing, which was carried out for up to 72h at RT. A large increase in the  
398 particle size was noticed only for the positively charged NPs (IC/PROT WMRs of 0.2 and  
399 0.5, Figure 7A) with a very rapid growth in the particle size and flocculation measured for the  
400 formulation with an IC/PROT WMR of 0.5. NPs with IC/PROT WMRs of 2 and 4 showed only  
401 a small increase in the particle size upon the storage. Interestingly, the increase in the  
402 hydrodynamic size of the IC/PROT WMR of 0.5 system after 24h was not accompanied by  
403 an increase in Pdl (Figure 7B). A gradual decrease in ZP values for NPs with a IC/PROT  
404 WMR of 0.5 was observed, indicative of PROT detachment (Figure 7C). The best colloidal  
405 stability was determined for NPs with WMRs of 2 and 4.

406 NPs with a positive surface charge (IC/PROT WMRs of 0.2 and 0.5) were physically  
407 unstable and aggregated either immediately after mixing with the medium (acetate buffer  
408 pH=4.5 and PBS pH=7.4) or extensive aggregation was observed after 24h (0.01M HCl and  
409 HEPES buffer pH=6.5) (Figure 8A and B). In contrast, good colloidal stability was seen for all

410 negatively charged formulations (IC/PROT WMPs of 2 and 4) with relatively small variations  
411 in the particle size recorded over time (Figure 8C and D).

412 As the component in excess charge-stabilises the PEC complex (PROT for NPs with positive  
413 surface charge and CAR for NPs with negative surface charge), its ability to remain on the  
414 surface in a range of conditions will define the colloidal stability of particles. As PROT  
415 comprises small, approximately 5 kDa fragments, this component can be easily removed  
416 from the particle surface, resulting in physical destabilisation of the system. On the other  
417 hand, CAR has approximately 100 times greater molecular weight and long, unbranched  
418 chains can form entangled structures and thus are removed with more difficulty. Moreover,  
419 the impact of the ionic strength of a medium on the binding constant is well known and  
420 mathematically presented by the “Record-Lohman” equation, which describes a double  
421 logarithmic dependence of the binding constant on the ionic strength (Record, Anderson and  
422 Lohman, 1978). Thus in electrolyte media the stability of polyelectrolyte complexes may be  
423 even further decreased, as shown in Figure 8.

424

#### 425 **4. Conclusions**

426 In this study, we have demonstrated that carrageenans could be used as suitable polymers  
427 for the formation of novel NPs via polyelectrolyte complexation with PROT. The type (KC, IC  
428 or LC) and solution concentration of carrageenans used was of particular importance. When  
429 0.1% w/v solutions were used, aggregation was seen for KC/PROT, while small nanoplexes  
430 with sizes of approximately 100-150 nm were obtained for the IC/PROT combination. The  
431 addition of calcium and zinc ions to the environment during the NP formation was seen to  
432 increase the particle size and surface potential of particulates and this may be perceived as  
433 an undesirable effect. Polyelectrolyte complexation was confirmed as the mechanism of NP  
434 formation accompanied by deformation of polysaccharide chains for IC/PROT systems.  
435 Good colloidal stability was seen for NPs with negative surface charge stored as native  
436 dispersions and with media at various pH.

437 IC was found to be the most suitable type of CAR, forming NPs with PROT that were  
438 smallest in size and most stable. Furthermore, the ease of formulation and mild preparative  
439 conditions required for preparation of these nanoplexes make them promising candidates in  
440 terms of use as nanocarriers. Therefore it is proposed to use IC/PROT nanoplexes for  
441 further studies involving loading of bioactive compounds for the purpose of drug delivery.

442

#### 443 **Acknowledgements**

444 This study was funded by Merrion Pharmaceuticals Ireland. This work was also supported by  
445 the Synthesis and Solid State Pharmaceutical Centre funded by Science Foundation Ireland  
446 under grant number 12/RC/2275. The authors would like to acknowledge the Imaging Core  
447 Facility, UCD Conway Institute of Biomolecular and Biomedical Research for performing  
448 TEM analysis.

449

#### 450 **Conflict of interest**

451 The authors declare that there are no conflicts of interest.

452

#### 453 **References**

454 Arman, M. & Qader S. A. U. (2010). Structural analysis of kappa-carrageenan isolated from  
455 *Hypnea musciformis* (red algae) and evaluation as an elicitor of plant defense mechanism.  
456 *Carbohydrate Polymers*, 88, 1264-1271.

457 Awotwe-Otoo, D., Agarabi, C., Keire, D., Lee, S., Raw, A., Yu, L., Habib, M. J., Khan, M. A.  
458 & Shah, R. B. (2012). Physicochemical characterization of complex drug substances:  
459 evaluation of structural similarities and differences of protamine sulfate from various sources.  
460 *AAPS Journal*, 14, 619-626.

461 Bayat, A., Dorkoosh, F. A., Dehpour, A. R., Moezi, L., Larijani, B., Junginger, H. E. & Rafiee-  
462 Tehrani, M. (2008). Nanoparticles of quaternized chitosan derivatives as a carrier for colon

463 delivery of insulin: ex vivo and in vivo studies. *International Journal of Pharmaceutics*, 356,  
464 259–266.

465 Berth, G., Vukovic, J. & Lechner, M. D. (2008). Physicochemical characterisation of  
466 carrageenans - a critical reinvestigation. *Journal of Applied Polymer Science*, 110, 3508-  
467 3524.

468 Bertoluzza, A., Fagnano, C., Finelli, P., Morelli, M. A., Simoni R. & Tosi R. (1983). Raman  
469 and infrared spectra of spermidine and spermine and their hydrochlorides and phosphates  
470 as a basis for the study of the interactions between polyamines and nucleic acids. *Journal of*  
471 *Raman Spectroscopy*, 14, 386–394.

472 Birch, N. P. & Schiffman, J. D. (2014). Characterization of self-assembled polyelectrolyte  
473 complex nanoparticles formed from chitosan and pectin. *Langmuir*, 30, 3441-3447.

474 Boddohi, S., Killingsworth, C. E. & Kipper, M. J. (2008). Polyelectrolyte multilayer assembly  
475 as a function of pH and ionic strength using the polysaccharides chitosan and heparin.  
476 *Biomacromolecules*, 9, 2021–2028.

477 Briones, A. V. & Sato, T. (2010). Encapsulation of glucose oxidase (GOD) in polyelectrolyte  
478 complexes of chitosan-carrageenan. *Reactive and Functional Polymers*, 70, 19–27.

479 Campo, V. L., Kawano, D. F., Braz da Silva, J. R. D. & Carvalho, I. (2009). Carrageenans:  
480 biological properties, chemical modifications and structural analysis - a review. *Carbohydrate*  
481 *Polymers*, 77, 167-180.

482 Chen, J. H., Heitmann, J. A. & Hubbe, M. A. (2003). Dependency of polyelectrolyte complex  
483 stoichiometry on the order of addition. 1. Effect of salt concentration during streaming current  
484 titrations with strong poly-acid and polybase. *Colloids and Surfaces A*, 223, 215-230.

485 Cundall, R. B., Lawton, J. B., Murray, D. & Phillips, G. O. (1979). Interaction of acridine  
486 orange and polyanions: fluorimetric determination of binding strengths and the influence of  
487 simple electrolytes. *Journal of the Chemical Society, Perkin Transactions*, 2, 879-884.

488 Dai, W. G., Dong, L. C. & Song, Y. Q. (2007). Nanosizing of a drug/carrageenan complex to  
489 increase solubility and dissolution rate. *International Journal of Pharmaceutics*, 342, 201-  
490 207.

491 Daniel-da-Silva, A. L., Trindade, T., Goodfellow, B. J., Costa, B. F., Correia, R. N., Gil, A. M.  
492 (2007). In situ synthesis of magnetite nanoparticles in carrageenan gels.  
493 *Biomacromolecules*, 8:2350-2357.

494 Delie, F. & Blanco-Prieto, M. (2005). Polymeric particulates to improve oral bioavailability of  
495 peptide drugs. *Molecules*, 10, 65–80.

496 Dodgson, K. S. & Price, R. G. (1962). A note on the determination of the ester sulphate  
497 content of sulphated polysaccharides. *Biochemical Journal*, 8, 106–110.

498 Dragan, E. S., Mihai, M. & Schwarz, S. (2006). Polyelectrolyte complex dispersions with a  
499 high colloidal stability controlled by the polyion structure and titrant addition rate. *Colloids  
500 and Surfaces A*, 290, 213–221.

501 Gu, Y. S., Decker, E. A. & McClements, D. J. (2004). Influence of pH and iota-carrageenan  
502 concentration on physicochemical properties and stability of beta-lactoglobulin-stabilized oil-  
503 in-water emulsions. *Journal of Agricultural and Food Chemistry*, 52, 3626-3632.

504 Gupta, V. K. & Karar, P. K. (2011). Optimisation of process variables for the preparation of  
505 chitosan-alginate nanoparticles. *International Journal of Pharmacy and Pharmaceutical  
506 Sciences*, 3, 1-3.

507 Hans, M. L. & Lowman, A. M. (2002). Biodegradable nanoparticles for drug delivery and  
508 targeting. *Current Opinion in Solid State and Materials Science*, 6, 319-327.

509 Hu, Y., Yang, T. & Hu, X. (2012). Novel polysaccharide-based nanoparticle carriers prepared  
510 by polyelectrolyte complexation for protein delivery. *Polymer Bulletin*, 6, 1183-1199.

511 Li, C., Hein, S. & Wang, K. (2013). Chitosan-carrageenan polyelectrolyte complex for the  
512 delivery of protein drugs. *ISRN Biomaterials*, Article ID 629807, doi:10.5402/2013/629807.

513 Liu, Z., Jiao, Y., Wang, Y., Zhou, Ch. & Zhang, Z. (2008). Polysaccharides-based  
514 nanoparticles as drug delivery systems. *Advanced Drug Delivery Reviews*, 60, 1650-1662.

515 Malafaya, P. B., Silva, G. A. & Reis, R. L. (2007). Natural-origin polymers as carriers and  
516 scaffolds for biomolecules and cell delivery in tissue engineering applications. *Advanced*  
517 *Drug Delivery Reviews*, 59, 207-233.

518 Melo, M. R. S., Feitosa, J. P. A., Freitas A. L. P. & de Paula R. C. M. (2002). Isolation and  
519 characterization of soluble sulfated polysaccharide from the red seaweed *Gracilaria cornea*.  
520 *Carbohydrate Polymers*, 49, 491-498.

521 Nanaki, S., Karavas, E., Kalantzi, L. & Bikiaris, D. (2010). Miscibility study of carrageenan  
522 blends and evaluation of their effectiveness as sustained release carriers. *Carbohydrate*  
523 *Polymers*, 79, 1157-1167.

524 Necas, J. & Bartosikova, L. (2013). Carrageenan: a review. *Veterinarni Medicina*, 58, 187-  
525 205.

526 Paluch, K. J., Tajber, L., McCabe, T., O'Brien, J. E., Corrigan, O. I. & Healy, A. M. (2010).  
527 Preparation and solid state characterisation of chlorothiazide sodium intermolecular self-  
528 assembly suprastructure. *European Journal of Pharmaceutical Sciences*, 41, 603-611.

529 Record, M. T. Jr., Anderson, C. F. & Lohman, T. M. (1978). Thermodynamic analysis of ion  
530 effects on the binding and conformational equilibria of proteins and nucleic acids: the roles of  
531 ion association or release, screening, and ion effects on water activity. *Quarterly Reviews of*  
532 *Biophysics*, 11, 103–178.

533 Reynolds, F., Weissleder, R. & Josephson, L. (2005). Protamine as an efficient membrane-  
534 translocating peptide. *Bioconjugate Chemistry*, 16, 1240-1245.

535 Ryan, S. M., McMorow, J., Umerska, A., Patel, H. B., Kornerup, K. N., Tajber, L., Murphy,  
536 E. P., Perretti, M., Corrigan, O. I. & Brayden, D. J. (2013). An intra-articular salmon  
537 calcitonin-based nanocomplex reduces experimental inflammatory arthritis. *Journal of*  
538 *Controlled Release*, 167, 120-129.

539 Sarmiento, B., Bibeiro, A., Veiga, F., Ferreira, D. & Neufeld, R. (2007). Oral bioavailability of  
540 insulin contained in polysaccharide nanoparticles. *Biomacromolecules*, *8*, 3054-3060.

541 Sarmiento, B., Ribeiro, A., Veiga, F. & Ferreira, D. (2006). Development and characterisation  
542 of new insulin containing polysaccharide nanoparticles. *Colloids and Surfaces B*, *53*, 193-  
543 202.

544 Shumilina, E. V. & Shchipunov, Y. A. (2002). Chitosan-carrageenan gels. *Colloid Journal*,  
545 *64*, 372–378.

546 Sonia, T. A. & Sharma, Ch. P. (2012). An overview of natural polymers for oral insulin  
547 delivery. *Drug Discovery Today*, *17*, 784-792.

548 Temsamani, J. & Vidal, P. (2004). The use of cell-penetrating peptides for drug delivery.  
549 *Drug Discoveries & Therapeutics*, *9*, 1012-1019.

550 Thrimawithana, T. R., Young, S., Dunstan, D. E. & Alany, R. G. (2010). Texture and  
551 rheological characterisation of kappa and iota carrageenan in the presence of counter ions.  
552 *Carbohydrate Polymers*, *82*, 69-77.

553 Thrimawithana, T. R., Young, S. A., Bunt, C. R., Geen, C. R. & Alany, R. G. (2011). In-vitro  
554 and in-vivo evaluation of carrageenan/methylcellulose polymeric systems for transscleral  
555 delivery of macromolecules. *European Journal of Pharmaceutical Sciences*, *44*, 399-409.

556 Umerska, A., Paluch, K. J., Inkielewicz-Stepniak, I., Santoz-Martinez, M. J., Corrigan, O. I.,  
557 Medina, C. & Tajber, L. (2012). Exploring the assembly process and properties of novel  
558 cross-linker free hyaluronate-based polyelectrolyte complex nanocarriers. *International*  
559 *Journal of Pharmaceutics*, *436*, 75-87.

560 Umerska, A., Paluch, K. J., Santos-Martinez, M. J., Corrigan, O. I., Medina, C. & Tajber, L.  
561 (2014). Self-assembled hyaluronate/protamine polyelectrolyte nanoplexes: synthesis,  
562 stability, biocompatibility and potential use as peptide carriers. *Journal of Biomedical*  
563 *Nanotechnology*, *10*, 3658-3673.

564 Yeo, Y., Baek, N. & Park, K. (2001). Microencapsulation methods for delivery of protein  
565 drugs. *Biotechnology and Bioprocess Engineering*, 6, 213-230.



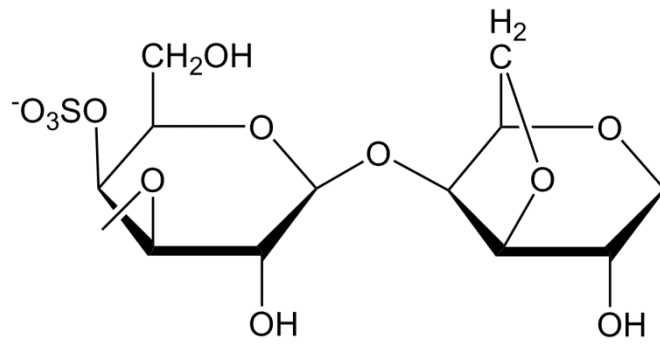
Table 1 Physicochemical properties of carrageenans and their solutions studied in this work.

KC – kappa carrageenan, IC – iota carrageenan, LC – lambda carrageenan.

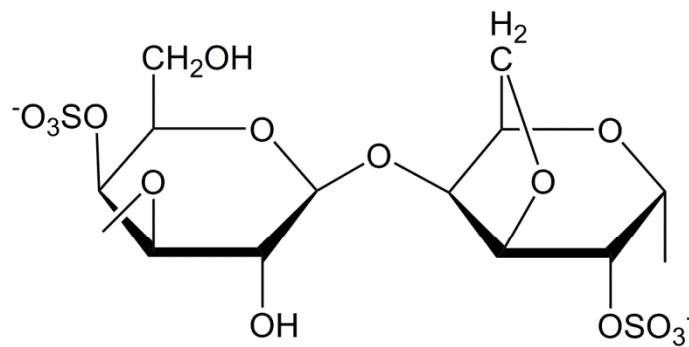
Polymer	Molecular weight (kDa)	Loss on drying (%)	Sulphate content (%)	Viscosity (mPa·s) of solution	pH of solution
KC	672±39	11.3±0.8	20.3±1.4	0.05% - 3.62±0.13 0.1% - 5.49±0.04	0.05% - 6.7±0.1 0.1% - 7.2±0.2
IC	724±175	18.1±0.4	26.6±1.2	0.05% - 2.63±0.05 0.1% - 4.34±0.01	0.05% - 6.3±0.0 0.1% - 6.6±0.1
LC	579±22	14.1±1.2	21.3±0.9	0.05% - 4.58±0.06 0.1% - 6.06±0.19	0.05% - 7.2±0.2 0.1% - 7.9±0.2

Table 2 FTIR band positions (in  $\text{cm}^{-1}$ ) in carrageenans, protamine (PROT) and nanoparticle (NP) formulations. The number in parenthesis indicate the magnitude of the shift in  $\text{cm}^{-1}$ , \* indicates that the group in NP formulation shifted by at least  $10 \text{ cm}^{-1}$ . KC – kappa carrageenan, IC – iota carrageenan, LC – lambda carrageenan,  $\nu$  – stretching,  $\nu_{s,a}$  – symmetric and asymmetric stretching,  $\nu_a$  – asymmetric stretching.

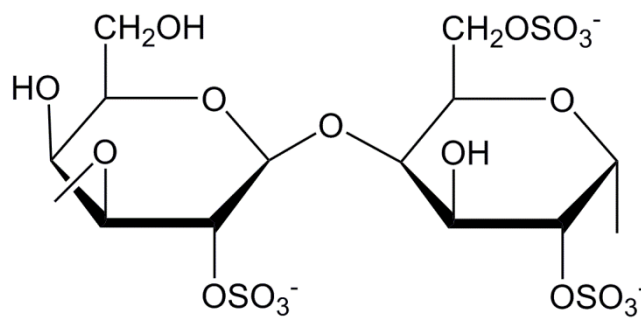
Band	KC	IC	LC	PROT	KC/PROT NPs	IC/PROT NPs	LC/PROT NPs
$\nu(\text{C-O}, \text{C-OH})$	1037	1024	1011	-	1033 (4)	1024 (0)	1007 (3)
$\nu_a(\text{COC})$	1157	1155	1154	-	1155 (2)	1161 (6)	1153 (1)
$\nu_{a,s}(\text{SO})$	1228	1215	1219	-	1212 (16)*	1215 (0)	1209 (10)*
$\nu_a(\text{SO}_2)$	1374	1373	1372	-	1363 (11)*	1375 (2)	1363 (9)
amide II and $\text{NH}_3^+$	-	-	-	1538	1535 (3)	1538 (0)	1534 (4)
amide I	-	-	-	1633	1647 (14)*	1645 (12)*	1651 (18)*



kappa carrageenan (KC)



iota carrageenan (IC)



lambda carrageenan (LC)

Figure 1. Chemical structure of kappa carrageenan (KC), iota carrageenan (IC) and lambda carrageenan (LC).

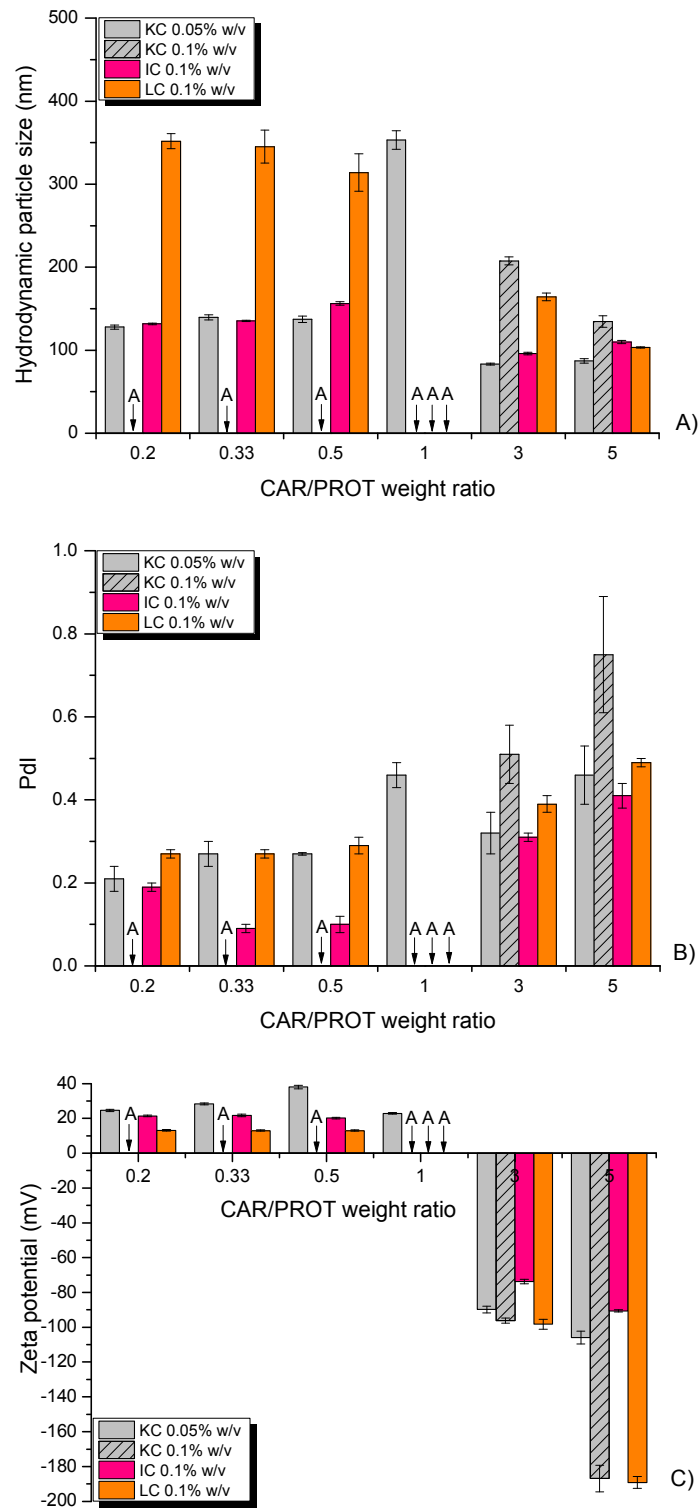


Figure 2. A) Hydrodynamic particle size, B) polydispersity index (Pdl) and C) zeta potential for NPs composed of various types of carrageenans and protamine (PROT). A – instantaneous aggregation, KC – kappa carrageenan, IC – iota carrageenan and LC – lambda carrageenan.

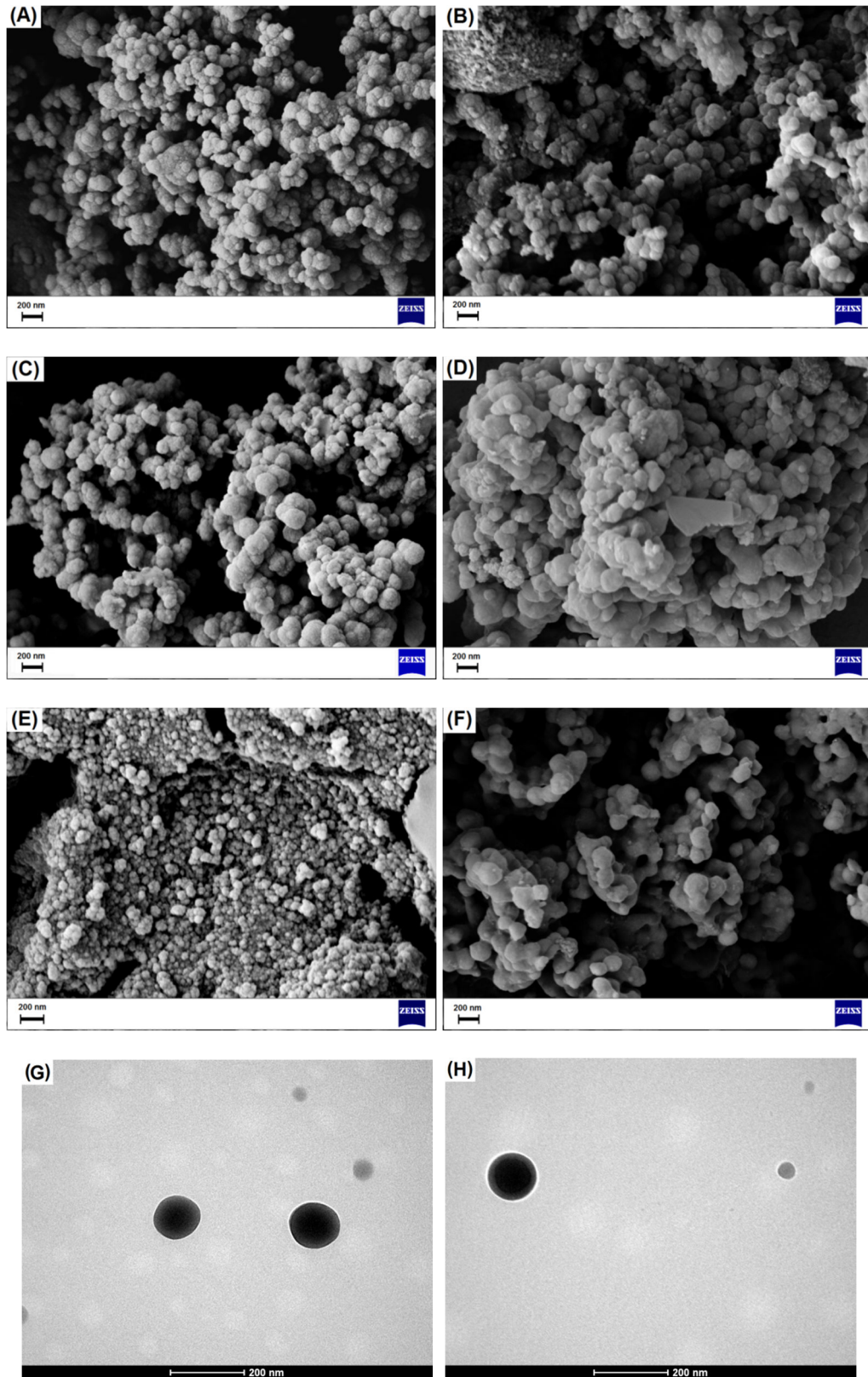


Figure 3. Electron micrographs: A) SEM of KC/PROT NPs with a WMR of 0.33, B) SEM of KC/PROT NPs with a WMR of 3, C) SEM of IC/PROT NPs with a WMR of 0.33, D) SEM of IC/PROT NPs with a WMR of 3, E) SEM of LC/PROT NPs with a WMR of 0.33, F) SEM of

LC/PROT NPs with a WMR of 3, G) TEM of IC/PROT NPs with a WMR of 0.5 and H) TEM of IC/PROT NPs with a WMR of 4. The concentration of constituents was 1 mg/ml. WMR - weight mixing ratio. KC – kappa carrageenan, IC – iota carrageenan, LC – lambda carrageenan and PROT – protamine.

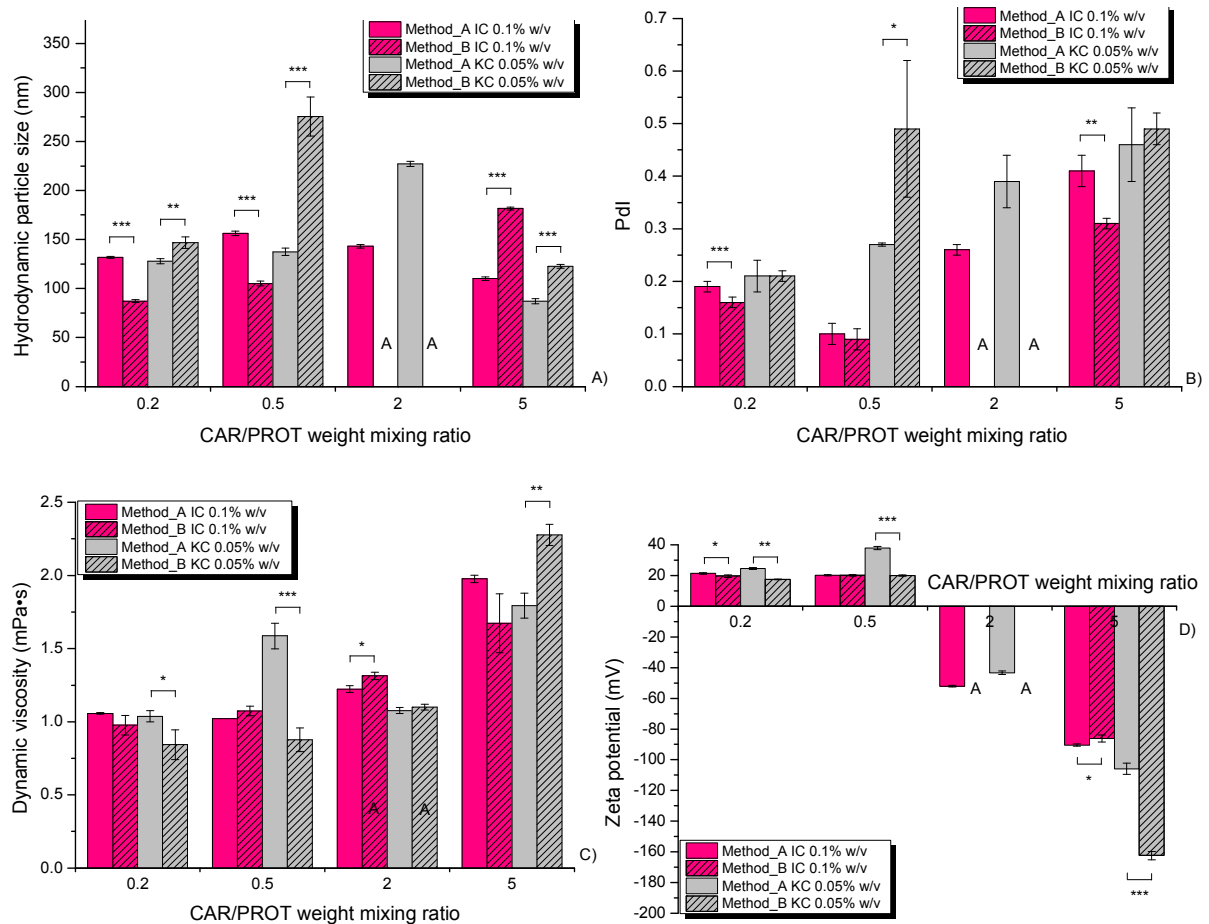


Figure 4. Comparison of: A) hydrodynamic particle size and B) polydispersity index (Pdl), C) dynamic viscosity and D) zeta potential for selected NPs composed of kappa carrageenan/protamine (KC/PROT, 0.05% w/v) and iota carrageenan/PROT (0.1% w/v) formed by the following variation in the method of preparation: Method\_A: an aliquot of PROT solution was added to an aliquot of carrageenan solution under magnetic stirring and Method\_B: an aliquot of carrageenan solution was introduced to an aliquot of PROT solution under magnetic stirring. A - instantaneous aggregation, statistical analysis: \* $p < 0.05$ , \*\* $p < 0.01$ , \*\*\* $p < 0.001$ .

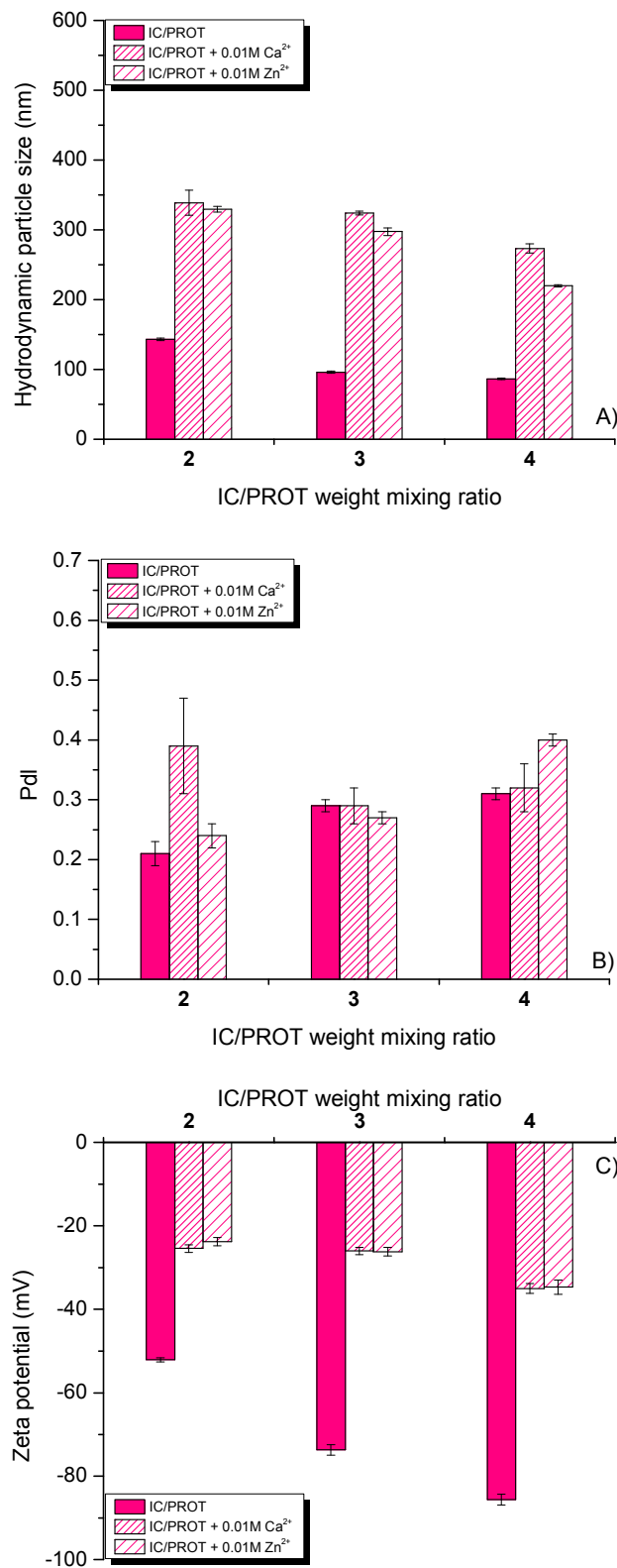


Figure 5. Comparison of: A) hydrodynamic particle size, B) polydispersity index (Pdl) and C) zeta potential values for NPs composed of iota carrageenan (IC) and protamine (PROT) without/with addition of calcium and zinc cations.

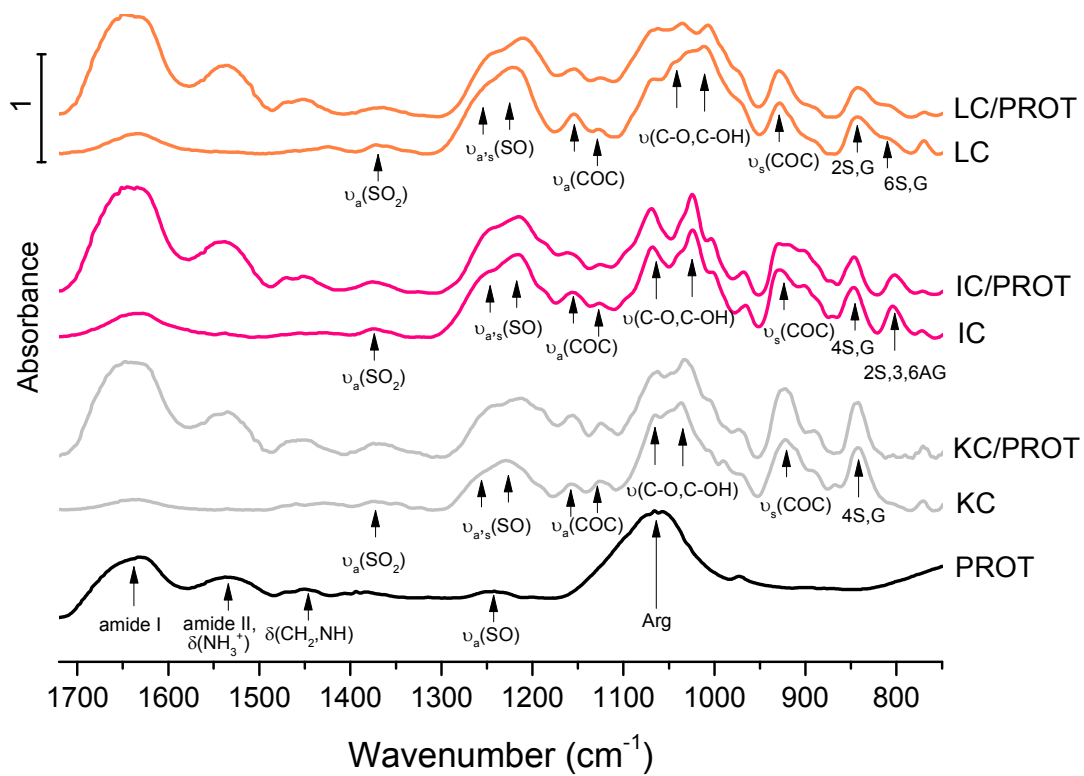


Figure 6. FTIR analysis of PROT, KC, IC, LC, KC/PROT NPs, IC/PROT NPs and LC/PROT NPs. Band assignment was done based on studies of Bertoluzza et al. (1983); Melo, Feitosa, Freitas and de Paula (2002); Nanaki, Karavas, Kalantzi and Bikiaris, (2010); Awotwe-Otoo et al. (2012); Arman & Quader (2012).  $\nu$  – stretching,  $\nu_{s,a}$  – symmetric and asymmetric stretching,  $\nu_s$  – symmetric stretching,  $\nu_a$  – asymmetric stretching and  $\delta$  – bending vibrations. Arg – arginine, 2S,G - 2-sulphate galactose (LC only), 4S,G - 4-sulphate galactose (KC and IC only), 6S,G - 6-sulphate galactose (LC only) and 2S,3,6AG - 2-sulphate 3,6-anhydrogalactose (IC only). KC – kappa carrageenan, IC – iota carrageenan, LC – lambda carrageenan and PROT – protamine.

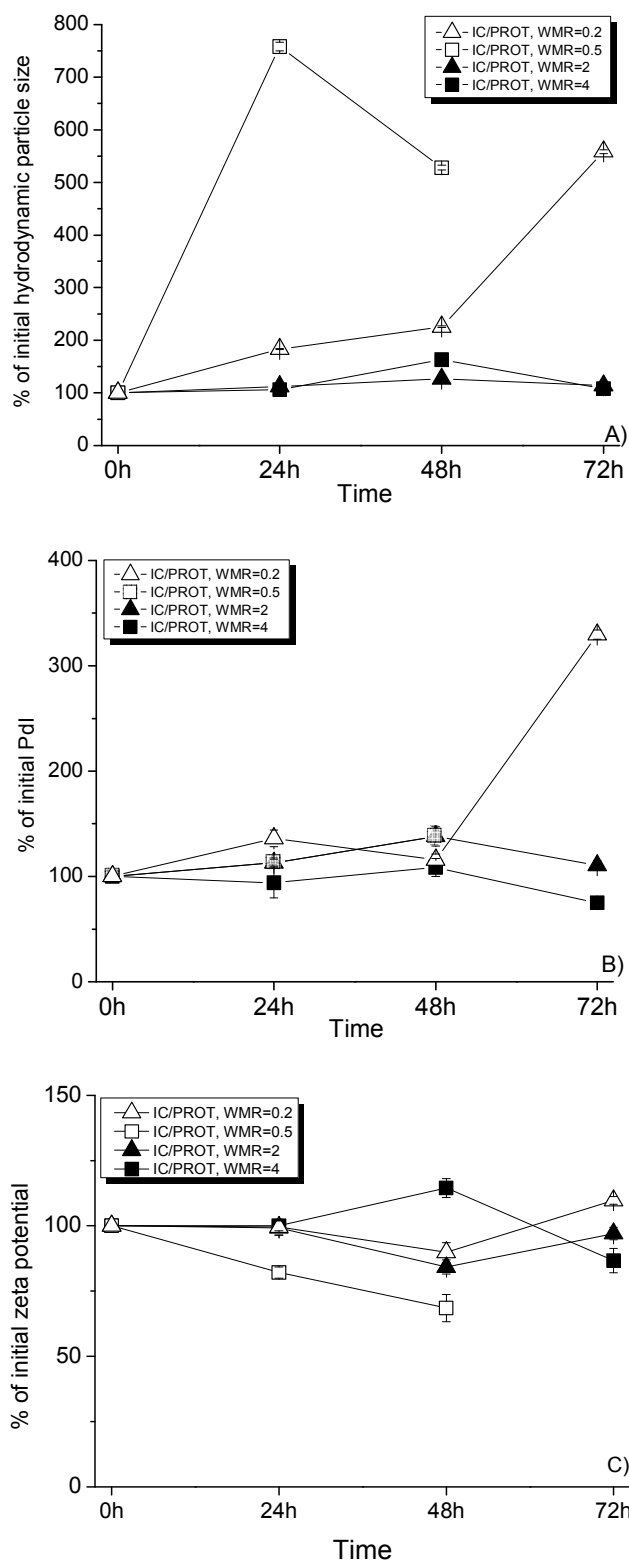


Figure 7. Colloidal stability studies of IC/PROT nanoparticle native dispersions at room temperature: A) hydrodynamic particle size, B) polydispersity index (Pdl) and C) zeta potential. WMR – weight mixing ratio, IC – iota carrageenan and PROT – protamine.



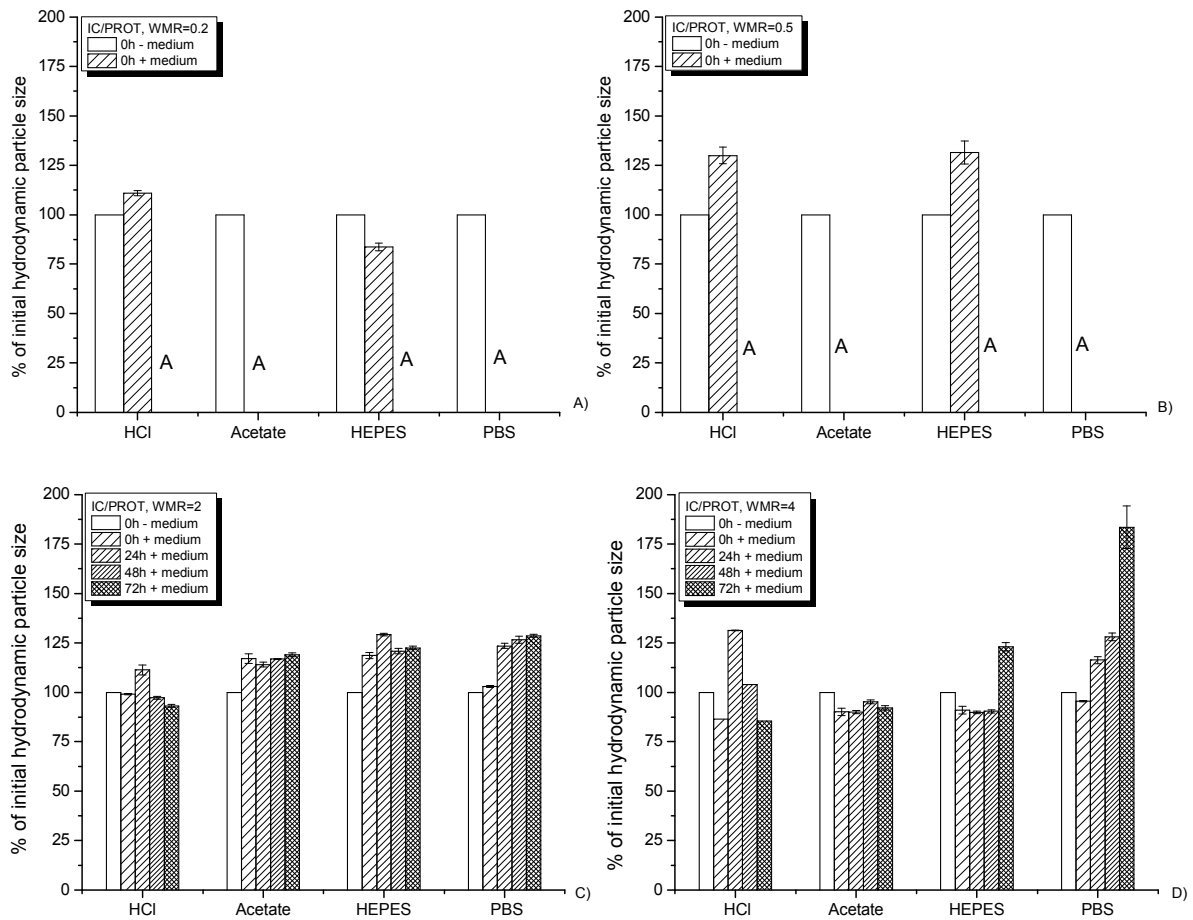


Figure 8. Colloidal stability studies based on monitoring hydrodynamic particle size changes of IC/PROT nanoparticle dispersions in media with various pH. The weight mixing ratios (WMRs) of IC/PROT were: A) 0.2, C) 0.5, D) 2 and F) 4. A – aggregation, IC – iota carrageenan and PROT – protamine, HCl – 0.01M HCl, Acetate - 0.1M acetate buffer pH 4.5, HEPES - 0.1M HEPES buffer pH 6.5 and PBS - 0.01M PBS pH=7.4.